Biochimica et Biophysica Acta 1840 (2014) 3190–3197

Contents lists available at ScienceDirect

Biochimica et Biophysica Acta

journal homepage: www.elsevier.com/locate/bbagen

Chemistry of free radicals produced by oxidation of endogenous α-aminoketones. A study of 5-aminolevulinic acid and α-aminoacetone by fast kinetics spectroscopy

P. Morlière [a,b,c,*], G.L. Hug [d], L.K. Patterson [b,d], J.-C. Mazière [a,b,e], J. Ausseil [a,b,e], J.-L. Dupas [e,f], J.-P. Ducroix [e,g], R. Santus [b,h], P. Filipe [i]

[a] INSERM, U1088, 80054 Amiens, France
[b] CHU Amiens, Pôle Biologie, Pharmacie et Santé des Populations, Centre de Biologie Humaine, Laboratoire de Biochimie, 80054 Amiens, France
[c] Université de Picardie Jules Verne, UFR de Pharmacie, 80036 Amiens, France
[d] University of Notre Dame, Radiation Laboratory, Notre Dame, IN 46556, USA
[e] Université de Picardie Jules Verne, UFR de Médecine, 80036 Amiens, France
[f] CHU Amiens, Service d'Hépato-Gastroentérologie, 80054 Amiens, France
[g] CHU Amiens, Service de Médecine Interne et Maladies Systémiques, 80054 Amiens, France
[h] Muséum National d'Histoire Naturelle, Département RDDM, 75231 Paris, France
[i] Hospital de Santa Maria, Faculdade de Medicina de Lisboa, Clínica Dermatologica Universitaria and Unidade de Investigação em Dermatologia, Instituto de Medicina Molecular, 1699 Lisboa Codex, Portugal

ARTICLE INFO

Article history:
Received 22 April 2014
Received in revised form 24 June 2014
Accepted 2 July 2014
Available online 10 July 2014

Keywords:
5-Aminolevulinic acid
α-Aminoacetone
Horse spleen ferritin
Human serum albumin
Antioxidants
Pulse radiolysis

ABSTRACT

Background: Excess 5-aminolevulinic acid (ALA) and α-aminoacetone (AA) are implicated in ketosis, porphyrinpathies and diabetes. Pathologic manifestations involve $^{\bullet}O_2^-$, H_2O_2, $^{\bullet}OH$, enoyl radicals ($^{\bullet}$ALA and $^{\bullet}$AA) and their oxidation end products.
Methods: To characterize enoyl radicals resulting from reaction of $^{\bullet}OH$ radicals with ALA and AA, micromolar $^{\bullet}OH$ concentrations were produced by pulse radiolysis of ALA and AA in aqueous solutions.
Results: ALA and AA react with $^{\bullet}OH$ at $k = 1.5 \times 10^9\ M^{-1}\ s^{-1}$. At pH 7.4, the $^{\bullet}$ALA absorbance spectrum has a maximum at 330 nm ($\varepsilon = 750\ M^{-1}\ cm^{-1}$). This band appears as a shoulder at pH 8.3 where two ALA species are present: $(NH_3)^+$-CH_2-CO-CH_2-CH_2-COO^- and NH_2-CH_2-CO-CH_2-CH_2-COO^- (pKa = 8.3). At pH 8.3, $^{\bullet}$ALA reacts with oxygen ($k = 1.4 \times 10^8\ M^{-1}\ s^{-1}$) but not with $^{\bullet}O_2^-$. At pH 8.3, AA oxidation produces two $^{\bullet}$AA species characterized by an absorbance spectrum with maxima at 330 and 450 nm. $^{\bullet}$ALA and $^{\bullet}$AA are repaired by antioxidants (quercetin (QH), catechin, trolox, ascorbate) which are semi-oxidized ($k > 10^8\ M^{-1}\ s^{-1}$). QH bound to HSA or to apoferritin and ferritin repairs $^{\bullet}$ALA and $^{\bullet}$AA. In O_2-saturated apoferritin solutions, $^{\bullet}$Q, $^{\bullet}O_2^-$, $^{\bullet}$AA and reaction product(s) react with QH.
Conclusions: The optical absorption properties and the time evolution of $^{\bullet}$ALA and $^{\bullet}$AA were established for the first time. These radicals and their reaction products may be neutralized by antioxidants free in solution or bound to proteins.
General significance: Adjuvant antioxidant administration may be of interest in pathologies related to excess ALA or AA production.

1. Introduction

The metabolism of amino acids in humans can be dramatically perturbed as a consequence of inborn or acquired enzyme deficiencies. As a consequence, accumulation of an essential metabolite among those involved in key metabolic pathways may occur. Such an imbalance can affect locally or in a systemic manner the function of essential organs. In this article, we focus on two α-aminoketones (AKs) involved in the normal metabolism of amino acids, namely, 5-aminolevulinic acid (ALA) and α-aminoacetone (AA) (see scheme 1). 5-Aminolevulinic acid is a heme precursor which accumulates in hepatic porphyrias and in

Abbreviations: apoFt, apoferritin; Ft, ferritin; SOD, superoxide dismutase; HSA, human serum albumin; AK, α-aminoketone; ALA, 5-aminolevulinic acid; AA, α-aminoacetone; G, radiolytic yield; AH^-, ascorbate; QH, quercetin; CatH, catechin; TrOH, trolox®

* Corresponding author at: CHU Amiens Sud, Pôle Biologie, Pharmacie et Santé des Populations, Centre de Biologie Humaine–Biochimie Recherche, INSERM U 1088, Avenue René Laennec, Salouël, 80054 Amiens Cedex 1, France. Tel.: +33 3 22 08 70 18; fax: +33 3 22 08 70 59.
E-mail address: morliere.patrice@chu-amiens.fr (P. Morlière).

http://dx.doi.org/10.1016/j.bbagen.2014.07.002
0304-4165/

tyrosinemia [1–3]. Excess ALA provokes acute neurological disorders and is implicated in a high incidence of hepatoma [4]. α-Aminoacetone is a threonine catabolite which accumulates in diseases characterized by high levels of circulating threonine such as threoninemia and the "cri-du-chat" syndrome [5]. Most importantly, excess AA is thought to be a source of methylglyoxal, a potent reagent of DNA bases and protein residues [3]. Both AKs are characterized by the presence of methylene groups adjacent to the carbonyl. α-Aminoacetone and ALA have one and two methylene groups, respectively. With such structural characteristics, these molecules undergo a rapid enolization catalyzed by phosphate ions at physiological pH. In the case of ALA, enolization occurs predominantly at C-5 [6]. These enols can donate one electron to oxygen by subsequent transition metal ion-catalyzed oxidation reactions in oxygenated media [3]. It has been proposed that, besides enoyl radical formation, these reactions produce superoxide radical anions and hence H_2O_2 which generate strongly reactive $^{\bullet}OH$ radicals by Fenton-like reactions [3,7].

It is therefore of interest to characterize the enoyl radical species ($^{\bullet}$ALA and $^{\bullet}$AA) formed by the reactions of $^{\bullet}OH$ radicals with ALA and AA. For these measurements, micromolar concentrations of $^{\bullet}OH$ radicals have been selectively produced by pulse radiolysis of buffered aqueous solutions of ALA and AA. Pulse radiolysis is a fast spectroscopic technique which provides spectral characterization as well as time-dependent behavior of radical species [8]. In N_2O-saturated solutions $^{\bullet}OH$ radicals can be produced alone although $^{\bullet}OH$ radicals and $^{\bullet}O_2^-$ radicals are produced simultaneously in O_2-saturated solutions. As the $^{\bullet}$ALA and $^{\bullet}$AA radicals are thought to play a role in the physiopathology of diseases mentioned above, it is important to examine the potential neutralization of these harmful radicals by antioxidants. Representative molecules from several families of antioxidants, namely, the hydrophobic flavone QH and the hydrophilic flavanol catechin (CatH), the vitamin E analog, trolox® (TrOH), and the ascorbate anion (AH^-) were selected for this model study.

2. Materials and methods

2.1. Chemicals and routine equipment

All inorganic chemicals were of analytical grade and were used as received from the suppliers. 5-Aminolevulinic acid and AA were supplied by Santa Cruz Biotechnology (Santa Cruz, CA, USA). Superoxide dismutase from bovine erythrocytes (SOD), horse spleen Ft and apoferritin (apoFt), delipidated human serum albumin (HSA), QH, CatH, TrOH and ascorbic acid were purchased from Sigma-Aldrich (St Louis, Mo, USA). Phosphate buffers were prepared in pure water obtained with a reverse osmosis system from Ser-A-Pure Co. The water from this system exhibited a resistivity of >18 MΩ cm^{-1} and a total organic content of <10 ppb. Absorption spectrophotometry was carried out in quartz cells with an Uvikon 922 spectrophotometer.

2.2. Pulse radiolysis

Pulse radiolysis measurements were performed with the Notre Dame Radiation Laboratory 8-MeV linear accelerator, which generates 5 ns pulses of up to 30 Gy. In general, the doses used in this work were ~20 Gy. The detection system, previously described [9,10], allows one to follow reaction kinetics in time domains up to 15 ms after the radiolytic pulse in the 290–700 nm spectral range. The radiolytic dose was determined using as a dosimeter the transient absorbance of the $^{\bullet}(SCN)_2^-$ radical-anion measured immediately after the radiolytic pulse at 472 nm. For this dosimetry (10^{-2} M SCN^- in N_2O-saturated solution), a radical chemical yield (G) × ε value for $^{\bullet}(SCN)_2^-$ equal to 5.28×10^{-4} m^2 J^{-1} was assumed. The G value is defined as the radical concentration divided by the radiolytic dose and can be expressed as μM Gy^{-1} (or μmol J^{-1} in dilute solution). The G value for $^{\bullet}OH$ in N_2O-saturated solution has been measured as ~0.64 μM Gy^{-1} [11]. Experiments were performed at room temperature (20 °C).

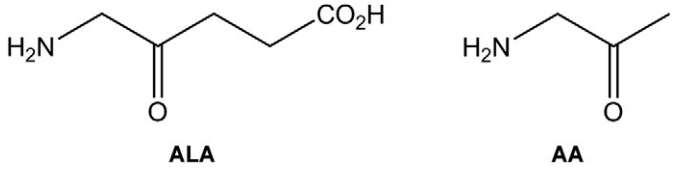

Scheme 1.

2.3. Preparation of the ALA and AA solutions for pulse radiolysis

The ALA and, to a lesser extent, AA rather readily auto-oxidize at mildly basic pH. Solutions (up to 5 mM) were therefore prepared in 0.1 M phosphate buffer (pH 8.3) at room temperature (20 °C) immediately before pulse radiolysis to avoid significant oxidation and/or dimerization (especially with ALA [6]) during the duration of a pulse radiolysis run (30 min or less). The pH drop (up to 1 unit), recorded after ALA solubilization in 0.1 M phosphate buffer (pH 8.8) was adjusted to pH 8.3 after stepwise addition of 1 M NaOH solution in water and the solutions were immediately saturated with pure N_2O. Some experiments were performed at pH 7.4 with 10 mM phosphate buffer.

2.4. Preparation of the Ft and apoFt solutions for pulse radiolysis

The Ft and apoFt stock solutions (48 mg mL^{-1}) from Sigma-Aldrich were delivered in 150 mM NaCl. Before pulse radiolysis measurements, these stock solutions were dialyzed twice against 1 L of pH 7.4 buffer. The dialyzed protein solutions were then diluted to the desired concentration assuming a molecular mass of ~440,000. An estimate of the Fe(III) content of Ft was obtained with the spectroscopic method developed by May and Fish [12] using the average value of the molar absorption coefficient given by Buettner et al. [13]. A solution containing 0.1 mg mL^{-1} leads to an absorbance of 0.23 at 380 nm. Thus, using ε(380 nm) = 19.0 ml $mg(Fe)^{-1}$ cm^{-1}, it was found that Ft contained ~1000 Fe(III) per molecule. Diluted solutions (up to 40 mL) were gently bubbled with the desired gas for 10 min prior to pulse radiolysis. To minimize the quantity of proteins consumed in each experiment, a micro-cell (optical path: 1 cm, volume: 120 μL) was used for transient recording. This micro-cell was emptied and refilled after each radiolytic pulse by a remote syringe pump to assure that all data were obtained with un-irradiated protein solutions. For the study of the effects of QH on protein radicals, 2 μM protein solutions were equilibrated for 2 h in the dark with aliquots of stock solutions of QH (10 mM in 0.1 M NaOH) to ensure full binding of the flavone to apoFt or Ft.

2.5. Analysis of kinetic data

Kinetics and spectral measurements were taken at least twice, and the results were found to be reproducible from day to day. Numerical integrations for analyses of complex rate data were carried out using Scientist software from Micromath Scientific Software. Rate constants were determined from raw data by the calculations with the above software.

3. Results and discussion

3.1. One-electron oxidation of AKs by $^{\bullet}OH$ radicals in N_2O- or O_2-saturated solutions

The sequence of reactions leading to the one-electron oxidation of AKs by $^{\bullet}OH$ radicals is as follows. The initial event is the radiolysis of water producing as main species: e_{aq}, $H^{\bullet}$, $^{\bullet}OH$, and H_2O_2. In N_2O-saturated solutions the hydrated electrons (e_{aq}) are converted into $^{\bullet}OH$ radicals by the reaction: $e_{aq} + N_2O + H_2O \dashrightarrow {}^{\bullet}OH + N_2 +$

OH^- [7]. Under these conditions, the G of the $^{\bullet}OH$ radicals is 0.64 μM Gy^{-1}. In O_2-saturated solutions hydrated electrons and hydrogen atoms are converted into $^{\bullet}O_2^-$ radical-anions by the reaction: e_{aq} (or $H^{\bullet}$) + $O_2 \rightarrow {}^{\bullet}O_2^-$ (or $^{\bullet}O_2^- + H^+$). At pH > 6, only $^{\bullet}O_2^-$ species are present in the solution as the pK_a of the $^{\bullet}HO_2$ radical is 4.8. The $^{\bullet}OH$ and $^{\bullet}O_2^-$ Gs are 0.32 μM Gy^{-1} and 0.34 μM Gy^{-1}, respectively. Under both conditions, $^{\bullet}$AK radicals are readily formed by the general reaction: $^{\bullet}OH + AK(H) \rightarrow {}^{\bullet}AK + H_2O$ where (H) indicates a hydrogen atom on the carbon next to the carbonyl function. The carbon-centered radical thus produced has been observed by spin trapping experiments during the aerobic oxidation of ALA [7]. It is believed to be associated with the hybrid resonant enoyl radical

R-C(O)-$^{\bullet}$CH-NH_2 ↔ R-C($^{\bullet}$O) = CH-NH_2.

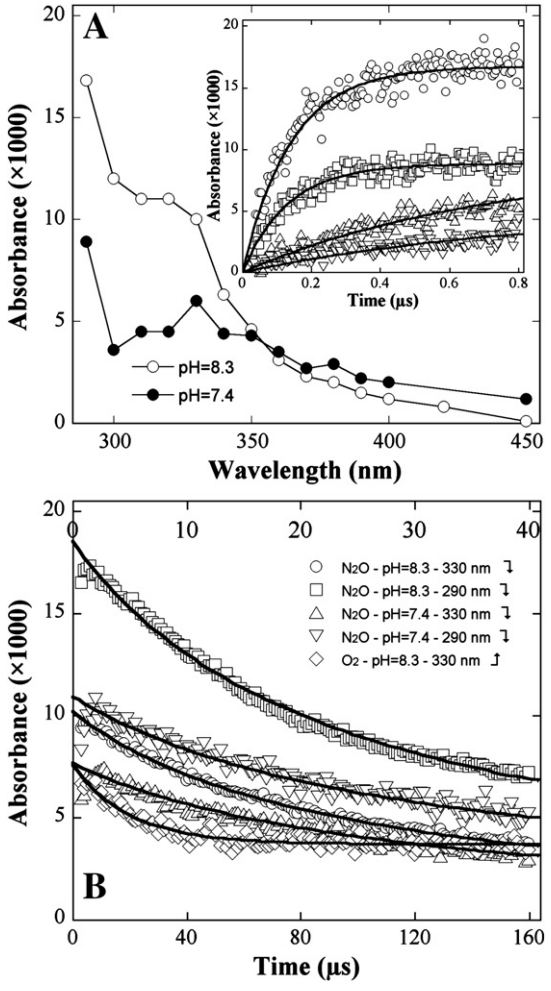

Fig. 1. A. Transient absorbance spectra observed after pulse radiolysis of 1 mM ALA in N_2O-saturated solutions pH 7.4, 10 mM phosphate buffered solution (●) or pH 8.3, and 0.1 M phosphate buffered solution (○). The transient absorbance spectra were recorded 2 μs after the radiolytic pulse. Dose per pulse was 19 Gy (●) or 21 Gy (○). Inset: Growth kinetics recorded at 290 nm (○) and 330 nm (□, △, ▽) after pulse radiolysis of 5 mM (○, □) or 1 mM (△, ▽) ALA in N_2O-saturated pH 8.3, 0.1 M phosphate buffered solution (○, □, △) or pH 7.4, 10 mM phosphate buffered solution (▽). Solid lines correspond to fitted data. Dose per pulse was 20 Gy. B. Lower time scale (↴): decay kinetics measured at 290 nm (□, ▽) and 330 nm (○, △) after pulse radiolysis of 1 mM ALA in N_2O-saturated pH 8.3, 0.1 M phosphate buffered solution (○, □) or pH 7.4, 10 mM phosphate buffered solution (△, ▽). Upper time scale (↥): decay kinetics measured after pulse radiolysis of 1 mM ALA in O_2-saturated pH 8.3, 0.1 M phosphate buffered solution (◊). Solid line corresponds to fitted data. The absorbance measured under O_2-saturation was multiplied by 2 for better comparison with N_2O-saturated solution. Dose per pulse was 20 Gy in all cases.

3.1.1. Characteristics of $^{\bullet}$ALA radicals produced by reaction of ALA with $^{\bullet}OH$ radicals

Fig. 1A shows the transient absorbance spectra obtained with ALA solutions 2 μs after the radiolytic pulse under two pH and ionic strength conditions. In N_2O-saturated solutions at pH 7.4, the transient absorbance spectrum of the $^{\bullet}$ALA radicals had a well-resolved absorption maximum at 330 nm whereas at pH 8.3, the 330 nm band appeared as a shoulder in the transient spectrum. These spectral differences are probably explained by the oxidation by $^{\bullet}OH$ radicals of two different ALA species whose concentration is governed by the ionic equilibrium: $H_2O + (NH_3)^+$-CH_2-CO-CH_2-CH_2-$COO^- \rightleftarrows NH_2$-$CH_2$-CO-$CH_2$-$CH_2$-$COO^- + H_3O^+$ whose pKa is 8.3 [3]. Thus, at pH 7.4, the zwitterion was mainly present in the solution while the anion contributed to ~50% at pH 8.3. Furthermore, it has been demonstrated by NMR spectroscopy that two enol forms can co-exist [6]. Their formation is catalyzed by phosphate ions. At pH 8.3, they can be written as: NH_2-CH = C(OH)-CH_2-CH_2-COO^- (a) or NH_2-CH_2-C(OH) = CH-CH_2-COO^- (b). The NMR data demonstrated that (a) is by far the preponderant species, (b) being at a very small concentration [6]

The inset in Fig. 1A shows the kinetics of growth in the transient absorbance at 290 and 330 nm formed by the reaction

$$^{\bullet}OH + ALA(H) \rightarrow {}^{\bullet}ALA + H_2O. \quad (1)$$

Excellent concentration-dependent first order growths were observed (data not shown) from which bimolecular reaction rate constants $k_1 = 1.4 \times 10^9\ M^{-1}\ s^{-1}$ and $1.5 \times 10^9\ M^{-1}\ s^{-1}$ were determined for reaction (1) at pH 8.3 at 290 and 330 nm, respectively. The fair agreement between the k_1 values measured at these two wavelengths suggests that there was no modification of the $^{\bullet}$ALA species susceptible to induce spectral changes in the UV region on the 1 μs time scale. At pH 7.4 a similar k_1 value ($1.2 \times 10^9\ M^{-1}\ s^{-1}$) was determined reflecting comparable reactivity of $^{\bullet}OH$ radicals with the zwitterion and the anion.

Molar absorption coefficients (ε) were estimated assuming full $^{\bullet}OH$ scavenging by 5 mM ALA at pH 8.3 as suggested by data in the inset of Fig. 1A. These data led to ε = 750 M^{-1} cm^{-1} and ε = 1330 M^{-1} cm^{-1} at 330 and 290 nm, respectively. Under N_2O saturation, $^{\bullet}$ALA radicals decayed by a second-order process independent of the ALA concentration and of the observation wavelength (e.g. 290 or 330 nm) according to the reaction

$$2\,{}^{\bullet}ALA \rightarrow products. \quad (2)$$

characterized by 2 $k_2 = 7.6 \times 10^8\ M^{-1}\ s^{-1}$ and $6.6 \times 10^8\ M^{-1}\ s^{-1}$ at pH 8.3 and pH 7.4, respectively (Fig. 1B).

The agreement between these two rate constants supports the formation of a single $^{\bullet}$ALA radical species. The difference in the spectral shapes shown in Fig. 1A, is most probably due to substantial protonation of the amino group at pH 7.4, but there is no data available on the pk_a of the NH_3^+/NH_2 group of the radical species. There is no indication that new species strongly absorbing in the near UV region were produced by reaction (2).

The decay kinetics shown in Fig. 1B demonstrate that $^{\bullet}$ALA radicals readily reacted with O_2 since a strong increase in the decay rate was observed that may be attributed to the reaction

$$^{\bullet}ALA + O_2 \rightarrow product(s). \quad (3)$$

Assuming $[O_2] = 1.25$ mM under O_2-saturation, the bimolecular reaction rate constant $k_3 = 1.25 \times 10^8\ M^{-1}\ s^{-1}$ at pH 8.3, was calculated through the use of the Scientist software by taking into account the recombination reaction of $^{\bullet}$ALA radicals (reaction (2)) which occurred in parallel with the oxidation by O_2. It may be noted that the fairly effective reaction of $^{\bullet}$ALA radicals with oxygen led to the formation of a long-lived product absorbing in the near-UV region as shown by a remaining absorbance at the end of the decay (Fig. 1B). In addition, there was no indication on at least the 150 μs time scale of some reaction of

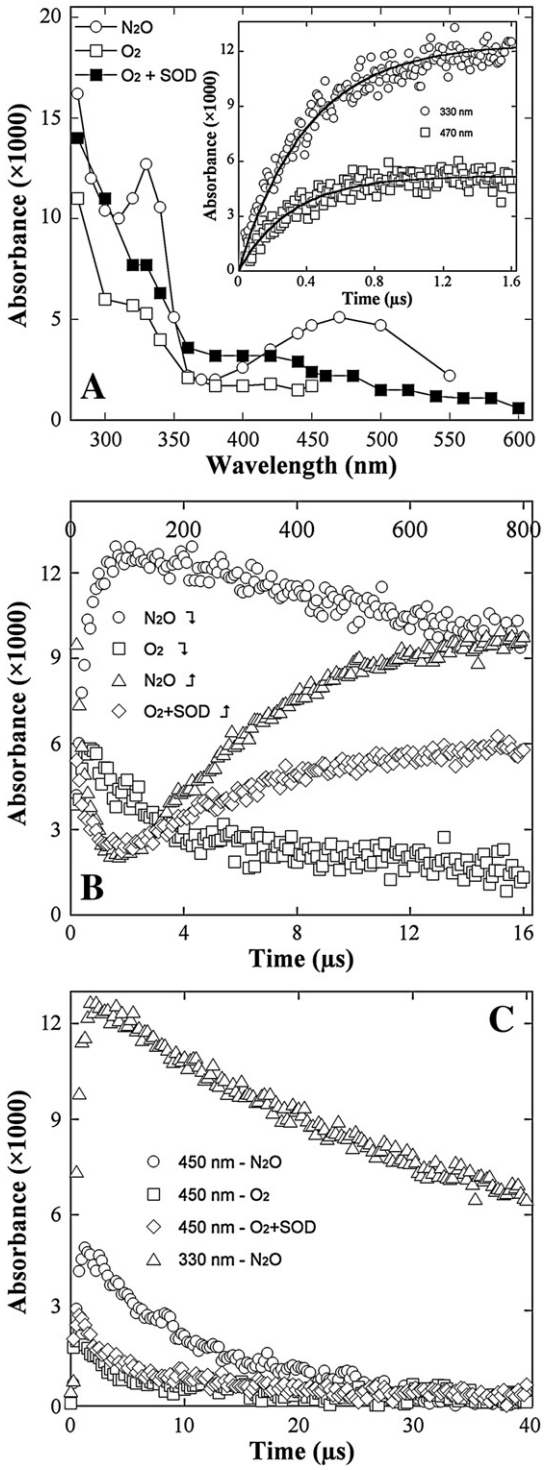

Fig. 2. A. Transient absorbance spectra observed 1 μs after pulse radiolysis of 2 mM AA (○) in N_2O-saturated pH 8.3, 0.1 M phosphate buffered solution. (□, ◊) same as before but in O_2-saturated solutions containing 2 mM AA (□) or 2 mM AA and 15 μM SOD (◊). Dose per pulse was 21 Gy (○, □) or 31 Gy (◊). Inset: Growth kinetics recorded at 330 nm (○) and 470 nm (□) after pulse radiolysis of 2 mM AA in N_2O-saturated pH 8.3, 0.1 M phosphate buffered solution. Dose per pulse was 20 Gy. Solid lines correspond to fitted data. B. Decay kinetics measured at 330 nm after pulse radiolysis of N_2O- (○, △) or O_2- (□, ◊) saturated pH 8.3, 0.1 M phosphate buffered solution containing 2 mM AA (○, △, □) or 2 mM AA and 15 μM SOD (◊). Lower time scale (○, □, ↴). Upper time scale (△, ◊, ↥). Dose per pulse was 21 Gy (○, △, □) or 31 Gy (◊). C. Decay kinetics measured at 330 nm (△) and 450 nm (○, □, ◊) after pulse radiolysis of N_2O- (○, △) or O_2- (□,◊) saturated pH 8.3, 0.1 M phosphate buffered solution containing 2 mM AA (○, △, □) or 2 mM AA and 15 μM SOD (◊). Dose per pulse was 21 Gy (○, △, □) or 31 Gy (◊).

ALA with the $^{\bullet}O_2^-$ radical-anions produced at a G (0.34 μM Gy^{-1}) similar to that of $^{\bullet}OH$ radicals (0.32 μM Gy^{-1}).

3.1.2. Characteristics of $^{\bullet}$AA radicals produced by reaction of AA with $^{\bullet}OH$ radicals

The inset in Fig. 2A suggests that in the 0.1 M phosphate buffer (pH 8.3) AA reacted with $^{\bullet}OH$ radicals at the diffusion-controlled rate. By analogy with ALA, this reaction is written as

$$^{\bullet}OH + AA(H) \rightarrow {}^{\bullet}AA + H_2O. \quad (4)$$

Accordingly, the $^{\bullet}$AA radical was produced by hydrogen abstraction of H atoms on the carbon next to the carbonyl function yielding the hybrid resonant enoyl radical [7]. Values of $k_4 = 1.3 \times 10^9\ M^{-1}\ s^{-1}$ and $1.6 \times 10^9\ M^{-1}\ s^1$ were calculated from the growth kinetics at 330 and 470 nm, respectively, fully consistent between them and comparable to k_1 measured with ALA.

In N_2O- or O_2-saturated buffered solutions containing 2 mM AA (pH 8.3), reaction (4) produced transient species whose transient absorptions observed 1 μs after the radiolytic pulse are shown in Fig. 2A. In the UV region, the spectrum of the $^{\bullet}$AA transient in N_2O-saturated solutions was rather similar to that obtained with $^{\bullet}$ALA with an absorbance maximum at 330 nm but the former exhibits an additional absorption band with a maximum at about 470 nm. The pKa of AA is 6.8 [3]; consequently, only uncharged species, mainly NH_2-CH_2-CO-CH_3, were present in solutions at pH 8.3. However, two enolic forms can co-exist in aqueous media, i.e. NH_2-CH = C(OH)-CH_3 or NH_2-CH_2-C(OH) = CH_2 in equilibrium with the ketone. However, in contrast with ALA [6] no NMR data concerning these equilibria are presently available in the literature. Apparent molar extinction coefficients of the $^{\bullet}$AA species were determined assuming full $^{\bullet}OH$ scavenging by 2 mM AA at pH 8.3. The data in the inset of Fig. 2A led to ε ~ 950 $M^{-1}\ cm^{-1}$ and ε ~ 450 $M^{-1}\ cm^{-1}$ at 330 and 470 nm, respectively.

The kinetics shown in Fig. 2B,C demonstrate that under N_2O saturation the 330 nm and 450 nm transient absorption bands decayed at different rates. Indeed, the $^{\bullet}$AA radical species decayed by second-order processes represented by the reaction

$$2\,{}^{\bullet}AA \rightarrow \text{products} \quad (5)$$

characterized by $2k_5 = 2.2 \times 10^9\ M^{-1}\ s^{-1}$ and $6.7 \times 10^9\ M^{-1}\ s^{-1}$ at 330 and 450 nm, respectively. This suggests that they originate from differing $^{\bullet}$AA species. It has been proposed that products of reaction (5) could result from a dismutation reaction restoring AA and forming the iminoAA(methylglyoxime) [14]. However, deamination of enoyl radicals may also occur since NH_4^+ is a product of AK autooxidation [3]. This observation is at variance with ALA for which only a single species was obtained upon oxidation by $^{\bullet}OH$. It should be noted that the k_6 constants are over-estimates as they were determined assuming the formation of a single $^{\bullet}$AA species.

A comparison of transient spectra obtained 1 μs after the pulse in the presence and in the absence of O_2 suggests a fast reaction of $^{\bullet}$AA radicals with O_2. As observed with ALA, a general decrease in the absorbance already occurred within 1 μs in the UV and more dramatically in the visible regions. Clear evidence for a fast reaction

$$^{\bullet}AA + O_2 \rightarrow \text{product(s)} \quad (6)$$

was also provided by decay kinetics recorded at several wavelengths under O_2 saturation on the 15 μs time scale (lower time scale in Fig. 2B) and on a longer time scale (40 μs) in Fig. 2C. Both figures suggest complex decay kinetics and thus complex oxidation paths occurring in competition with the recombination of $^{\bullet}$AA radicals (reaction (5)) with no significant SOD effect on the kinetics at either 450 nm (Fig. 2B) or 330 nm (data not shown). Unfortunately, the low transient absorptions at the relevant wavelengths and the existence of two different species contributing to reaction (5) precluded meaningful

determination of rate constants. These complex decays are possibly due to the parallel formation and decay of oxidation products of reaction (6) involving several •AA radical species that might be expected from the various equilibria which may take place in the solutions. Finally, the kinetics measured on the 800 μs time scale (Fig. 2B) reveal the slow formation of further product(s) (P) originating from the •AA recombination product(s). These P product(s) absorb in the UV, but their formation did not involve oxidation products of reaction (6) which occurred in competition with reaction (5) as the yield of the product(s) after 800 μs was ~50% lower in the presence of O_2 than in its absence (Fig. 2B). Indeed with the higher dose per pulse used in these O_2 experiments, the initial •OH concentration producing the •AA species was only somewhat less than 25% lower than that under N_2O.

3.2. Reactivity of AK enoyl radicals with electron donors

The •ALA and •AA radicals have been implicated in pathological processes [3,14–16]. It is therefore of interest to determine whether effective neutralization of •AK radicals by good electrons or hydrogen donors like antioxidants may be possible. The pulse radiolysis method is appropriate to check this hypothesis. Here the deactivation of •AK free radicals and/or toxic products due to their subsequent time evolution was evaluated with several antioxidants from different families. The hydrophobic QH and the water-soluble CatH of the flavonoid group, the water-soluble α-tocopherol substitute TrOH and AH^- were chosen in this study.

3.2.1. Evidence for one-electron reduction of •ALA and •AA radicals by antioxidants

Transient absorbance spectra and their main spectroscopic parameters, e.g. molar absorption coefficients, absorbance maxima (λ_{max}) of the one-electron oxidation product of QH (•Q), TrOH (TrO•), AH^- ($•A^-$), and CatH (Cat•) are well characterized as they have been the subject of extensive research [17–21]. Upon reaction with •ALA or •AA radicals, the time-dependent appearance of the characteristic transient absorbance of the one-electron oxidation product of the antioxidant was observed. Fig. 3 presents in N_2O-saturated buffered solutions (pH 8.3) the growth of absorbance measured at 550 nm ($\varepsilon = 9400\ M^{-1}\ cm^{-1}$) and 430 nm ($\varepsilon = 7100\ M^{-1}\ cm^{-1}$) corresponding to the λ_{max} of •Q and TrO•, respectively [17,18]. Depending on the antioxidant concentration (data not shown), the electron (or hydrogen) transfer from QH or TrOH to •ALA or •AA took place over 50–100 μs, compared to less than

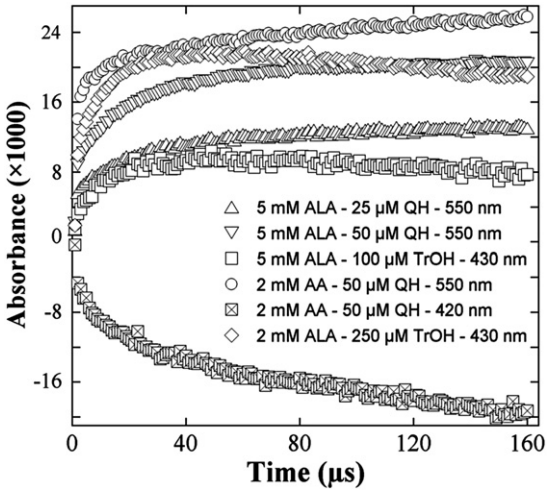

Fig. 3. Kinetics of absorbance growth of the •Q radicals at 550 nm (△, ▽, ○), and of the TrO• radicals at 430 nm (□, ◊) after pulse radiolysis of 5 mM ALA (△, ▽, □, ◊) or 2 mM AA (○, ⊠) in N_2O-saturated pH 8.3, 0.1 M phosphate buffered solution containing 25 μM QH (△), 50 μM QH (▽, ○, ⊠), 100 μM TrOH (□) or 250 μM TrOH (◊). The QH bleaching kinetics at 420 nm after pulse radiolysis of an N_2O- saturated pH 8.3, 0.1 M phosphate buffered solution containing 50 μM QH and 2 mM AA is shown in (⊠). Dose per pulse was 22 Gy.

1 μs for the •OH scavenging by ALA or AA (see insets Figs. 1A and 2A). This electron/hydrogen transfer can be represented by [17,19]

$$•ALA(or•AA) + QH(orTrOH) \rightarrow ALA(orAA) + •Q(orTrO•). \quad (7)$$

Consistent with reaction (7), Fig. 3 shows the parallel bleaching of QH at 420 nm ($\varepsilon_{QH} = 9400\ M^{-1}\ cm^{-1}$). This is a wavelength where the transient •Q absorbance becomes negligible [19]. Antioxidant consumption resulted from the electron/hydrogen transfer. Whenever possible, these transfer experiments were performed with at least a 50-fold excess of ALA (5 mM) or a 10-fold excess of AA (2 mM) as compared to the antioxidant concentration. This ratio of ALA and AA to antioxidant allowed for the scavenging of at least 80% of •OH radicals by ALA or AA; AH^- being most reactive with •OH radicals with a rate constant $1.1 \times 10^{10}\ M^{-1}\ s^{-1}$ [20,22]. Under our dose per pulse conditions (~20 Gy), the concentration of antioxidants – except that of the less water-soluble QH – was kept ~10 times higher than that of •OH radicals. All the antioxidants reacted with the •ALA and •AA radicals, the k_7 rate constants all exceeding $10^8\ M^{-1}\ s^{-1}$ (Table 1) as estimated from reasonably good pseudo first order growths (data not shown). The ascorbate anion was found to be a particularly effective inhibitor. However, it must be stressed that the k_7 values reported in Table 1 are only indicative as obtained with pseudo-first order fittings without taking into account the competition with radical–radical recombination reactions (2) and (5). Thus, in the case of AA, the decay of two independent •AA radical species produced by reaction with •OH radicals competed with reaction (7). It is noteworthy that the antioxidant effectiveness is correlated with the rate constant k_7 and not to the yields reported in Table 1 which are concentration-dependent. It should be mentioned that products resulting from further reactions of the primary •AA radicals can also be very effectively "repaired" by QH. Thus, the growth of the transient •Q absorbance and the parallel bleaching of QH took place over 500 μs (data not shown) at times when the primary •AA radicals had disappeared (see Fig. 2C).

Relatively low yields of "repair" of ALA and AA by electron/hydrogen transfer reactions are reported in Table 1. This may result from the concentration needed to avoid substantial •OH scavenging by the antioxidant and also from an over-estimate of the k_7 values (see above). The transfer yields were estimated as the ratio of the [•Q], [TrO•], [•Cat] or [$•A^-$], formed during the transfer, to the [•ALA] and [•AA] initially produced. The slow part of the transient absorbance growths similar to those shown in Fig. 3 were attributed to the electron/hydrogen transfer, taking into account any contributions from the fast absorbance rise as being due to the initial •OH scavenging by ALA, AA or the antioxidants. The [•ALA] and [•AA] initially produced were determined from the [•OH] produced by the radiolytic dose after correction for the proportion of •OH scavenging by the antioxidant (see [22] for relevant rate constants).

Table 1
Transfer rate constant (k_7) and transfer yield obtained after pulse radiolysis of 5 mM ALA or 2 mM AA in presence of antioxidants in N_2O-saturated pH 8.3, 0.1 M phosphate buffered solutions.

Conditions	k_7 ($10^8\ M^{-1}\ s^{-1}$)	Transfer yield[a] (%)
ALA + QH	8.1	9[b], 5[c]
ALA + CatH	6.1	8[b], 5[c]
ALA + TrOH	1.9	26[b], 13[c]
ALA + AH^-	24	12[b], 6[c]
AA + QH	2.8	15
AA + TrOH	4.0	8[d]

[a] Observation wavelengths: •Q at 550 nm ($\varepsilon = 9400\ M^{-1}\ cm^{-1}$), TrO• at 430 nm ($\varepsilon = 7100\ M^{-1}\ cm^{-1}$), •Cat at 310 nm ($\varepsilon = 9400\ M^{-1}\ cm^{-1}$) and •A at 360 nm ($\varepsilon = 9400\ M^{-1}\ cm^{-1}$).
[b] [QH] = 50 μM, [CatH] = 200 μM, [TrOH] = 500 μM or [AH^-] = 200 μM.
[c] [QH] = 25 μM, [CatH] = 100 μM, [TrOH] = 100 μM or [AH^-] = 100 μM.
[d] [TrOH] = 250 μM.

3.2.2. Neutralization of ˙ALA and ˙AA radicals by QH bound to proteins

Under physiological conditions, hydrophobic antioxidants may be bound to transport proteins. Thus one may examine to which extent the kinetic parameters of the repair reactions of ˙ALA and ˙AA radicals by QH free in solution are modified upon binding to its natural transporter, e.g. HSA. Furthermore, the pivotal role played by ˙ALA and ˙AA radical species in Fe(II) mobilization from Ft has been suggested in previous non-time dependent studies [3,15]. As we previously showed that QH could bind to apoFt and Ft [23], we also examined a possible protective role of QH in preventing apoFt and Ft from the oxidative damage induced by ˙ALA and ˙AA radicals.

3.2.2.1. Interaction of ˙ALA and ˙AA radicals with HSA-bound QH. In humans, the main conjugates resulting from QH metabolism are glucuronides, sulphates and the 3′-O-methyl derivative Their antioxidant activity is comparable or superior to that of QH [24]. Since thermodynamic data are available only for the HSA–QH complex formation, it is a good model to study ˙AK repair attributable to HSA-bound flavonols.

Quercetin binds to a relatively inaccessible site in HSA [25] in plasma with an equilibrium binding constant of $2.6 \times 10^5\ M^{-1}$ as reported by Boulton et al. [26] and confirmed by Filipe et al. [27]. In a N_2O-saturated solution containing 25 μM HSA and 25 μM QH (Fig. 4), the concentration of free QH (QH_f) is 8 μM whereas that of bound QH (QH_b) is 17 μM. These concentrations were chosen to minimize direct ˙OH scavenging by HSA (rate constant: $7.8 \times 10^{10}\ M^{-1}\ s^{-1}$ [22]) in the presence of 5 mM ALA or 3 mM AA. Furthermore, ˙AK radicals may not react with the most oxidizable amino acid residues since Trp, Tyr and Cys free in solution were unreactive with ˙ALA radicals (data not shown).

Complex kinetics reflecting the difference in reactivity between free and bound QH molecules may be expected. In Figs. 3 and 4, the kinetics of the absorbance growth at 550 nm, i.e. λ_{max} of ˙Q or the kinetics of QH bleaching at 410 or 420 nm were compared. Time scales in Fig. 4 suggest that the rates of transfer characterizing the electron/hydrogen transfer reaction (reaction (7)) from QH_b to ˙ALA and ˙AA radicals free in solutions were about an order of magnitude slower than those of free QH (Fig. 3). The QH bleaching shown in Fig. 4 is consistent with a two-step process. The fast one may be attributed to both the repair of ˙AA radicals by QH_f and to the decay of the ˙AA radicals which notably absorb at 420 nm (see Fig. 2A). The slowest step involves the repair of ˙AA radicals by QH_b. Moreover, the transient absorbance change at 550 nm measured after 750 μs and 1.5 ms in the presence of HSA, for respectively ALA and AA (Fig. 4), was at least an order of magnitude smaller than those shown in Fig. 3 in the absence of HSA but measured after 150 μs although QH concentration is the same in both cases. It suggests that binding to its carrier markedly reduces the ability of QH to inhibit the potentially harmful ˙ALA and ˙AA radicals most probably because the radical–radical recombination reactions (2) and (5) compete with the transfer reaction (7) attributable to the rather inaccessible QH_b. Given the large QH molar extinction coefficients ($14{,}300\ M^{-1}\ cm^{-1}$ at 410 nm and $9400\ M^{-1}\ cm^{-1}$ at 420 nm at pH 7.4) as well as the small ˙Q absorbance in the 410–420 nm region ($<500\ M^{-1}\ cm^{-1}$ [19]), it is possible to get a rough estimate of the QH percentage (Φ) consumed at the end of reaction (7) with respect to the initial ˙OH concentration. In the case of AA, 0.15 ms after the radiolytic pulse, this Φ value was found to be ~1% (Fig. 4). This is consistent with the low transfer yield in HSA measured at 550 mm. It supports the premise of no QH consumption by other paths than reaction (7) and full ˙OH scavenging by 3 mM AA. For comparison, the same estimate from Fig. 3 obtained with 2 mM AA yields Φ ~ 15%, this value being fully consistent with the transfer yield measured at 550 nm (Table 1).

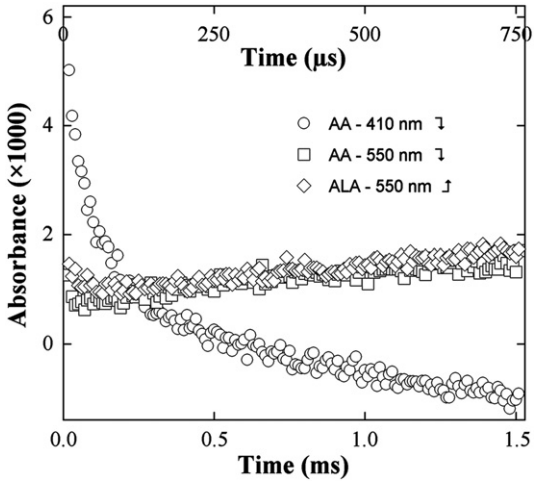

Fig. 4. Kinetics of absorbance change observed at 550 nm (□, ◊) and 410 nm (○) after pulse radiolysis of 5 mM ALA (◊) or 3 mM AA (□, ○) in N_2O-saturated pH 8.3, 0.1 M phosphate buffered solution containing 25 μM QH and 25 μM HSA. Upper time scale (◊, ↴), lower time scale (□, ○, ↴). Dose per pulse was 22 Gy.

3.2.2.2. Interaction of ˙ALA and ˙AA radicals with QH free or bound to apoFt and Ft. Ferritin – an essential protein responsible for iron storage in soluble and non-toxic form [28] – has been shown to be quite sensitive to harmful ˙AK radicals and to produce ROS [3,14–16]. It has recently been demonstrated that QH could partially repair oxidative damage inflicted to residues of apoFt or Ft [29]. In the current work, the putative protection brought by QH to apoFt and Ft, that have been subjected to ˙ALA and ˙AA radicals produced by ˙OH radicals, was also investigated either under N_2O-saturation or O_2-saturation as ROS are believed to play an important role in the apoFt and Ft oxidation induced by ALA and AA.

Quercetin binds to apoFt and Ft on 8 binding sites with apparent association constant K of ~80,000 M^{-1} and ~40,000 M^{-1}, respectively, reflecting a much weaker binding of QH to apoFt compared to that to HSA [23]. In experiments dealing with Figs. 5A,B and 6, the solutions contained 2 μM apoFt and 20 μM QH. Under these conditions, only 7.8 μM QH was bound to apoFt over 50% of the available sites.

In N_2O-saturated solutions (Fig. 5A,B), it can be observed that the kinetics of "repair" of ˙ALA by QH measured at 550 nm with apoFt were very different from those shown in Fig. 4 with HSA whereas the kinetics of bleaching measured at 410 nm indicate continuous QH depletion over 1.5 ms with Φ ~ 0.8%. In Ft solutions, reaction (7) was almost completely over after 50 μs at times corresponding to the "slow repair" attributed to QH_b. This result might suggest a fast deactivation of bound ˙Q_b by reactions involving the Fe^{3+} core. By contrast the kinetics obtained with AA in solutions containing either apoFt or Ft (Fig. 5B) are more understandable as ˙AA radicals still absorbed appreciably at 550 nm and their decay superimposed onto the ˙Q_f and/or the ˙Q_b growth. On the other hand, in the Ft solutions, at 550 nm, the "slow repair" was observed together with a fast absorbance decay observed at early times that may also bear some relationship with the Fe^{3+} core. Nevertheless, the complexity observed with the "repair" of ˙ALA and ˙AA probably arose from the large proportion of QH_f (60%) in the apoFt and Ft solutions, from the presence of multiple and non-equivalent QH binding sites and, possibly, from a decrease in the QH_b concentration upon QH_f consumption by virtue of the binding equilibrium. Moreover, molecular interactions of AKs with apoFt and Ft cannot be excluded whereas in the case of AA, the formation of several ˙AA species and decomposition products upon ˙OH radical attack must also be taken into account.

The processes described above were characterized under anoxic conditions, precluding any participation of O_2. Because of the obvious relationship to in vivo conditions and in view of previous literature reports, the effects of oxygen on reactions involved in the sequence of mechanisms discussed above were also investigated under aerobic conditions. Pulse radiolysis of an O_2-saturated solution produces $^{\cdot}O_2^-$ with $G = 0.34\ \mu M\ Gy^{-1}$ and ˙OH radicals with a $G = 0.32\ \mu M\ Gy^{-1}$.

It must first be noted as shown above that the $^{\cdot}O_2^-$ radical-anion does not react with ALA and AA, but it can directly oxidize QH by hydrogen

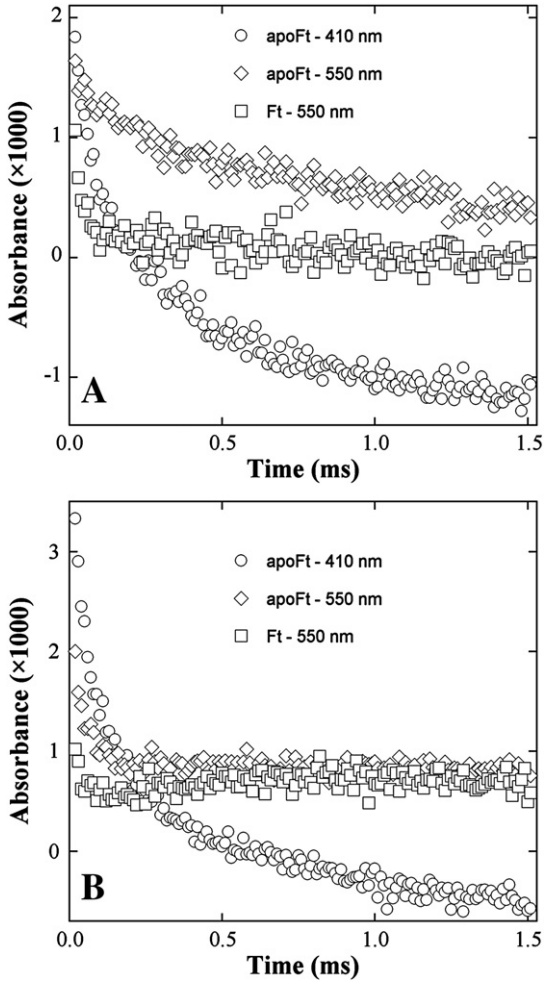

Fig. 5. A. Decay kinetics measured at 410 nm (○) and 550 nm (◊, □) after pulse radiolysis of N_2O-saturated pH 8.3, 0.1 M phosphate buffered solution containing 5 mM ALA, 20 μM QH and 2 μM horse spleen apoFt (○, ◊) or 2 μM horse spleen Ft (□). Dose per pulse was 21 Gy. B. Decay kinetics measured at 410 nm (○) and 550 nm (◊, □) after pulse radiolysis of N_2O-saturated pH 8.3, 0.1 M phosphate buffered solution containing 3 mM AA, 20 μM QH and 2 μM horse spleen apoFt (○, ◊) or 2 μM horse spleen Ft (□). Dose per pulse was 21 Gy.

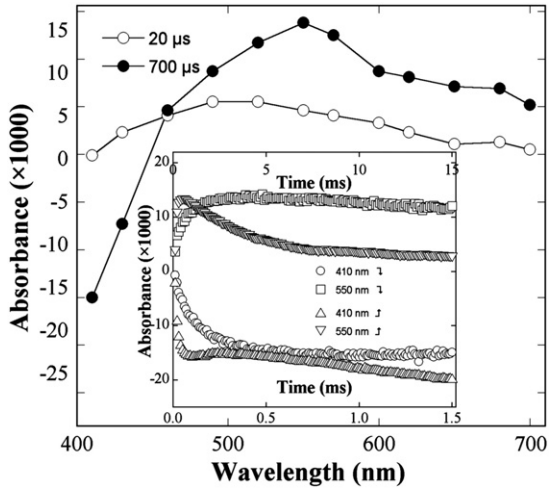

Fig. 6. Transient absorbance spectra observed 20 μs (○) and 700 μs (●) after pulse radiolysis of O_2-saturated pH 8.3, 0.1 M phosphate buffered solution containing 3 mM AA, 20 μM QH and 2 μM horse spleen apoFt. Dose per pulse was 31 Gy. Inset: Kinetics of absorbance change measured at 410 nm (○, △) and 550 nm (□, ▽) after pulse radiolysis of O_2-saturated pH 8.3, 0.1 M phosphate buffered solution containing 3 mM AA, 20 μM QH and 2 μM horse spleen apoFt. Lower time scale (○, □, ↴), upper time scale (△, ▽, ↾). Dose per pulse was 31 Gy.

abstraction or electron transfer followed by deprotonation with a rate constant $k_8 = 8 \times 10^5\ M^{-1}\ s^{-1}$ [19] according to

$$QH + {}^{\bullet}O_2^- + H^+ \rightarrow {}^{\bullet}Q + H_2O_2. \quad (8)$$

Fig. 6 presents the transient absorbance spectra recorded 20 μs and 700 μs after the radiolytic pulse in an O_2-saturated solution containing 3 mM AA, 20 μM QH and 2 μM apoFt at pH 8.3. Given that the initial $^{\bullet}OH$ concentration in an O_2-saturated solution is half that under N_2O-saturation and in view of the low absorbance shown by the kinetics in Fig. 5A,B, these spectra were recorded using a dose per pulse of 31 Gy to get more accurate data. Twenty microseconds after the pulse, the transient spectrum was clearly a superposition of the $^{\bullet}AA$ transient absorption (λ_{max} ~ 470 nm) with some contribution from the $^{\bullet}Q$ absorption. After 700 μs, this transient absorption was replaced by that of bound and free $^{\bullet}Q$ with the caveat that $^{\bullet}Q_b$ and $^{\bullet}Q_f$ have the same transient absorption. The growth and decay kinetics shown in the inset of Fig. 6 on different time scales clearly reveal several steps in the QH oxidation process. Thus, the 1.5 ms time scale suggests the occurrence of at least a fast plus a slower step presumably involving reactions (7) and (8). Taking as the initial concentration of the oxidizing radicals, the sum $[^{\bullet}OH] + [^{\bullet}O_2^-]$, Φ is found to be ~8%; that is to say much higher than that measured in N_2O-saturated solutions. This value supports QH oxidation by both AA and $^{\bullet}O_2^-$. Then, on the 15 ms time scale, another distinct reaction occurred from 1.5 ms to 15 ms as $^{\bullet}Q$ decayed with still a parallel QH consumption. Thus in this model system and in the presence of O_2, all radical species such as $^{\bullet}Q$, $^{\bullet}O_2^-$, and $^{\bullet}AA$ radicals as well as further reaction product(s) could be neutralized to the expense of QH.

4. Conclusions

The optical absorption properties and the time evolution of the transient radical species resulting from the oxidation of ALA and AA, two essential AKs, by $^{\bullet}OH$ radicals have been established for the first time. These radicals are likely formed by the abstraction of a hydrogen atom on the carbon next to the carbonyl function yielding the hybrid resonant enoyl radical [7]. The transient $^{\bullet}ALA$ and $^{\bullet}AA$ species have similar maximal absorption in the UV region at ~330 nm with molar extinction coefficients < 1000 $M^{-1}\ cm^{-1}$, but AA oxidation by $^{\bullet}OH$ radicals produces another weakly absorbing species absorbing at ~450 nm. No direct oxidation of these AKs by $^{\bullet}O_2^-$ could be observed although the $^{\bullet}O_2^-$ intervention has been suggested in the mechanistic interpretation of their aerobic auto-oxidation ([3] and references therein). Another interesting feature is the demonstration that $^{\bullet}ALA$ and $^{\bullet}AA$ were partially repaired by potent anti-oxidants such as CatH, TrOH, AH^- and QH, the latter being free in solution or bound to HSA or to apoFt and Ft. Moreover, studies in O_2-saturated solutions with QH suggest that not only reactive oxygen species and other radical intermediates but also reaction products of AK radicals are neutralized at the expense of the antioxidant. It might be speculated that these processes could be interesting ways to alleviate damage caused during oxidation of AKs. This is particularly relevant to physiological conditions as excess of both ALA and AA have been implicated in the loss of the antioxidant role of Ft and in the increase in iron overload leading to toxic pro-oxidant effects in rat brain, liver and other tissues susceptible to lesions like retina, kidneys and nerves accompanying chronic diseases such as diabetes or hepatic porphyries [3,16,29]. This work suggests some perspectives for exploring the potential benefits of an adjuvant administration of anti-oxidants in

ameliorating diseases related to acquired or inborn amino-acid metabolism impairment involving AKs.

Acknowledgements

This is document no. NDRL-5020 from the Notre Dame Radiation Laboratory which is supported by the Office of Basic Energy Sciences of the US Department of Energy through grant number DE-FC02-04ER15533.

References

[1] S. Sassa, Modern diagnosis and management of the porphyrias, Br. J. Haematol. 135 (2006) 281–292.
[2] J.T. Hindmarsch, The porphyrias: recent advances, Clin. Chem. 32 (1986) 1255–1263.
[3] E.J. Bechara, F. Dutra, V.E. Cardoso, A. Sartori, K.P. Olympio, C.A. Penatti, A. Adhikari, N.A. Assuncao, The dual face of endogenous alpha-aminoketones: pro-oxidizing metabolic weapons, Comp. Biochem. Physiol. C Toxicol. Pharmacol. 146 (2007) 88–110.
[4] R. Kauppinen, P. Mustajoki, Acute hepatic porphyria and hepatocellular carcinoma, Br. J. Cancer 57 (1988) 117–120.
[5] U. Kuhner, M. Busse, G. Buchinger, Cri-du-chat syndrome with an increased level of proline and threonine, Z. Kinderheilkd. 117 (1974) 259–264.
[6] A.R. Butler, S. George, The nonenzymatic cyclic dimerization of aminolevulinic acid, Tetrahedron 48 (1992) 7879–7886.
[7] H.P. Monteiro, D.S. Abdalla, O. Augusto, E.J. Bechara, Free radical generation during delta-aminolevulinic acid autoxidation: induction by hemoglobin and connections with porphyrinpathies, Arch. Biochem. Biophys. 271 (1989) 206–216.
[8] P. Wardman, Application of pulse radiolysis methods to study the reactions and structure of biomolecules, Rep. Prog. Phys. 41 (1978) 259–302.
[9] L.K. Patterson, J.A. Lilie, Computer-controlled pulse radiolysis system, Int. J. Radiat. Phys. Chem. 6 (1974) 129–141.
[10] G.L. Hug, Y. Wang, C. Schoneich, P.Y. Jiang, R.W. Fessenden, Multiple time scale in pulse radiolysis: applications to bromide solutions and dipeptides, Radiat. Phys. Chem. 54 (1999) 559–566.
[11] G.V. Buxton, C.R. Stuart, Reevaluation of the thiocyanate dosimeter for pulse radiolysis, J. Chem. Soc. Faraday Trans. 91 (1995) 279–281.
[12] M.E. May, W.W. Fish, The UV and visible spectral properties of ferritin, Arch. Biochem. Biophys. 190 (1978) 720–725.
[13] G.R. Buettner, M. Saran, W. Bors, The kinetics of the reaction of ferritin with superoxide, Free Radic. Res. Commun. 2 (1987) 369–372.
[14] A. Sartori, C.M. Mano, M.C. Mantovani, F.H. Dyszy, J. Massari, R. Tokikawa, O.R. Nascimento, I.L. Nantes, E.J. Bechara, Ferricytochrome (c) directly oxidizes aminoacetone to methylglyoxal, a catabolite accumulated in carbonyl stress, PLoS One 8 (2013) e57790.
[15] M.E. Rocha, F. Dutra, B. Bandy, R.L. Baldini, S.L. Gomes, A. Faljoni-Alario, C.W. Liria, M. T. Miranda, E.J. Bechara, Oxidative damage to ferritin by 5-aminolevulinic acid, Arch. Biochem. Biophys. 409 (2003) 349–356.
[16] F. Dutra, D. Araki, E.J. Bechara, Aminoacetone induces loss of ferritin ferroxidase and iron uptake activities, Free Radic. Res. 37 (2003) 1113–1121.
[17] S.V. Jovanovic, S. Steenken, M. Tosic, B. Marjanovic, M.G. Simic, Flavonoids as antioxidants, J. Am. Chem. Soc. 116 (1994) 4846–4851.
[18] M.J. Davies, L.G. Forni, R.L. Wilson, Vitamin E analogue Trolox C. E.S.R. and pulse-radiolysis studies of free-radical reactions, Biochem. J. 255 (1988) 513–522.
[19] S.V. Jovanovic, S. Steenken, M.G. Simic, Y. Hara, Antioxidant properties of flavonoids: reduction potentials and electronic transfer reactions of flavonoid radicals, in: C. Rice-Evans, L. Packer (Eds.), Flavonoids in Health and Disease, Marcel Dekker, New York, 1998, pp. 137–161.
[20] B.H.J. Bielski, D.A. Comstock, R.A. Bowen, Ascorbic acid free radicals. I. Pulse radiolysis study of optical absorption and kinetic properties, J. Am. Chem. Soc. 93 (1971) 5624–5629.
[21] S.V. Jovanovic, S. Steenken, Y. Hara, M.G. Simic, Reduction potentials of flavonoid and model phenoxy radicals. Which ring in flavonoids is responsible for antioxidant activity? J. Chem. Soc. Perkin Trans. 2 (1996) 2497–2504.
[22] G.V. Buxton, C.L. Greenstock, W.P. Helman, A.B. Ross, Critical review of rate constants for reactions of hydrated electrons, hydrogen atoms and hydroxyl radicals ($^{\bullet}OH/^{\bullet}O^{-}$) in aqueous solution, J. Phys. Chem. Ref. Data 17 (1988) 513–886.
[23] P. Morlière, J.C. Mazière, L.K. Patterson, M.A. Conte, J.L. Dupas, J.P. Ducroix, P. Filipe, R. Santus, On the repair of oxidative damage to apoferritin: a model study with the flavonoids quercetin and rutin in aerated and deaerated solutions, Free Radic. Res. 47 (2013) 463–473.
[24] C. Manach, C. Morand, V. Crespy, C. Demigné, O. Texier, F. Régérat, C. Rémésy, Quercetin is recovered in human plasma as conjugated derivatives which retain antioxidant properties, FEBS Lett. 426 (1998) 331–336.
[25] P. Filipe, P. Morlière, L.K. Patterson, G.L. Hug, J.-C. Mazière, C. Mazière, J.P. Freitas, A. Fernandes, R. Santus, Mechanisms of flavonoid repair reactions with amino acid radicals in models of biological systems: a pulse radiolysis study in micelles and human serum albumin, Biochim. Biophys. Acta 1572 (2002) 150–162.
[26] D.W. Boulton, U.K. Walle, T. Walle, Extensive binding of the bioflavonoid quercetin to human plasma proteins, J. Pharm. Pharmacol. 50 (1998) 243–249.
[27] P. Filipe, L.K. Patterson, D.M. Bartels, G.L. Hug, J.P. Freitas, J.-C. Mazière, R. Santus, P. Morlière, Albumin-bound quercetin repairs vitamin E oxidized by apolipoprotein radicals in native HDL_3 and LDL, Biochemistry 46 (2007) 14305–14315.
[28] P.M. Harrison, P. Arosio, The ferritins: molecular properties, iron storage function and cellular regulation, Biochim. Biophys. Acta 1275 (1996) 161–203.
[29] R. Demasi, C.A.A. Penatti, R. Delucia, E.J.H. Bechara, The prooxidant effect of 5-aminolevulinic acid in the brain tissue of rats: implications in neuropsychiatric manifestations in porphyrias, Free Radic. Biol. Med. 20 (1996) 291–299.